**Technical Annals**

Vol 1, No 6 (2024)

Technical Annals

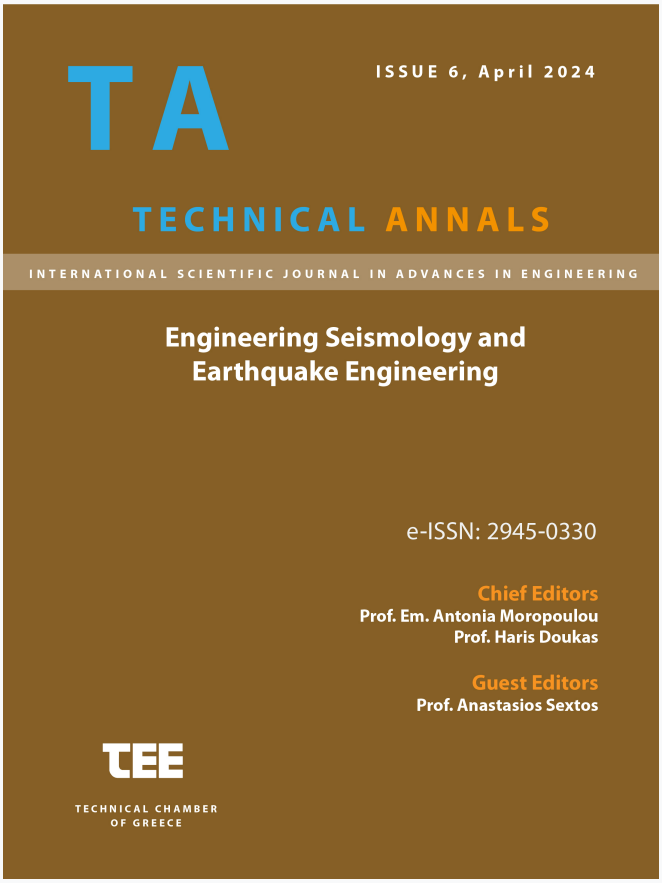


# Retrofit Strategies for Seismic Protection of Multi-Story Structures with Extended KDamper Devices

*Konstantinos Kapasakalis, Antonios Mantakas, Moris Kalderon, Evangelos Sapountzakis*

doi: 10.12681/ta.36870



**To cite this article:**

Kapasakalis, K., Mantakas, A., Kalderon, M., & Sapountzakis, E. (2024). Retrofit Strategies for Seismic Protection of Multi-Story Structures with Extended KDamper Devices. *Technical Annals*, *1*(6). https://doi.org/10.12681/ta.36870

# Retrofit Strategies for Seismic Protection of Multi-Story Structures with Extended KDamper Devices

K. Kapasakalis[1*] [0000-0002-6619-7374], A. Mantakas[1] [0000-0001-8136-5922], M. Kalderon[2] [0000-0002-1593-9892] and E.J. Sapountzakis[1]

[1]Institute of Structural Analysis and Antiseismic Research, School of Civil Engineering, National Technical University of Athens, Zografou Campus, GR-157 80 Athens, Greece
[2]Dynamics and Acoustics Laboratory, School of Mechanical Engineering, National Technical University of Athens, Zografou Campus, GR-157 80 Athens, Greece
kostiskapasakalis@hotmail.com*, mantakasantonis@gmail.com, cvsapoun@central.ntua.gr, moriska@mail.ntua.gr

**Abstract.** This paper evaluates the efficiency of the extended version of the KDamper (EKD) as a seismic retrofitting solution for existing multi-story building structures. Two distinct approaches are investigated. The first one considers the implementation of an EKD device at the structure's base level, a straightforward approach that simplifies the design process. The second one involves the dispersion of multiple EKDs throughout the height of the structure, a more computationally demanding approach, that aims to control higher modes, especially in high-rise structures. Three test cases are investigated, representing low, mid, and high-rise building structures. The primary objective is to provide insights into the effectiveness of each retrofitting strategy based on the structure's height and number of stories, presenting a comprehensive assessment of the advantages and disadvantages of each option. Overall, the results underscore the positive influence of the EKD system on the dynamic response of all examined multi-story structures, establishing it as a compelling technology for seismic retrofitting. Designers can compare different retrofitting strategies based on building height and number of stories to choose the most efficient option.

**Keywords:** Seismic Retrofitting, Damping, Negative Stiffness, KDamper.

## 1 Introduction

In recent years, seismic events have caused significant devastation, particularly in densely populated areas. Consequently, seismic regulations for buildings, bridges, and infrastructure have undergone changes to enhance their seismic performance. When it comes to the horizontal component of seismic forces, seismic isolation has emerged as a highly effective alternative to conventional seismic techniques. Unlike traditional methods that focus on increasing the structural capacity of constructions, seismic isolation operates by reducing seismic loads [1].

However, the application of seismic isolation at the base of structures inevitably leads to substantial displacements during seismic activity [2]. This drawback is not

universally acceptable due to various reasons. For instance, seismically isolated structures may be sensitive to wind loads, necessitate specific provisions for plumbing, heating, and drainage systems, and require substantial seismic joints to prevent collisions between neighboring buildings. These considerations render the seismic isolation approach unsuitable for existing structures.

The Tuned Mass Damper (TMD), a widely adopted method for passive vibration control, involves adding an oscillating mass, stiffness element, and damper to a structure. Introduced by Frahm [3] and optimized by Den Hartog [4], it was initially designed for undamped single-degree-of-freedom structures under harmonic excitations. While the TMD has shown improvements in dynamic behavior across various systems [5-16], it presents some drawbacks. Its efficiency depends on the optimum frequency and damping properties [17,18], and requires heavy masses, posing challenges in real applications. Moreover, seismic protection with a single TMD (STMD) may not be universally efficient due to the broad frequency spectrum of earthquakes [19,20].

To address the limitations of single TMD systems, researchers have proposed the use of multiple TMDs (MTMDs), either placed at the top floor or distributed across various levels (d-MTMDs). Initially introduced by Ayorinde and Warburton [21] for seismic control in civil engineering, MTMDs have been optimized by various researchers, showing increased efficiency compared to single TMDs, even when the total additional mass remains the same. The consensus is that optimizing the number of MTMDs expands the control frequency bandwidth. Recent research explores spatially distributed MTMDs to enhance the system's efficiency and to reduce the concentrated masses, as studied by Chen and Wu [22] on a six-story building structure.

A cutting-edge solution to these challenges comes in the form of the KDamper, developed in the National Technical University of Athens. This innovative approach relies on a meticulous combination of appropriate stiffness elements, including one with a negative stiffness constant [23,24]. The KDamper offers a unique advantage – the total stiffness of the superstructure can be maintained. This overcomes a key limitation of the "Quazi Zero Stiffness" (QZS) vibration isolation systems [25], which typically require a significant reduction in stiffness and, consequently, lead to decrease of the structure's load bearing capacity [26-29]. In comparison to traditional TMD, the KDamper achieves superior vibration absorption and damping characteristics without the need for additional heavy masses, a requirement that TMD has [30]. The KDamper stands out by replacing the high inertial forces of added masses with the force generated by the negative stiffness element [30-32]. Moreover, their isolation and damping properties primarily result from the stiffness elements of the system, making them less susceptible to issues like detuning, a challenge faced by conventional TMDs.

The effectiveness of the KDamper system has been explored for the protection of engineering structures against environmental loading, i.e bridges [33,34], wind turbines [35,36], and various other structural applications [24,37-40]. The mechanism has proven its ability to reduce displacement demands at the base level of seismically excited structures. In particular, Kapasakalis et al. [24] introduced the extended version of the KDamper concept (EKD) as a vibration absorber, while Mantakas et al. [38,41] examined the system's efficiency as a seismic retrofitting measure for low-rise buildings. In 2023, Kapasakalis et al. [42] introduced a multiple Extended KDamper (d-

EKD) approach to enhance the performance of retrofitting strategies. Similar to one of the d-Multiple Tuned Mass Dampers (d-MTMDs), this approach strategically places EKD devices between specified building floors. The study's findings indicated that the d-EKD devices outperformed d-MTMDs devices, achieving superior results with significantly less additional mass.

This study assesses the effectiveness of the EKD system as a seismic retrofitting measure for multi-storey structures. It explores two distinct approaches: the first involves employing an EKD as a seismic base absorber at the base level of the structure, while the second entails distributing multiple EKDs throughout the structure's height. Parametric analyses are carried out, considering factors such as the number of storeys and EKD devices. The overarching goal is to offer insights into the efficiency of each retrofitting strategy based on the structure's height and storeys, providing a comprehensive evaluation of the pros and cons of each option. In general, the findings highlight the positive impact of the EKD system on the dynamic response of all examined multi-storey structures, establishing it as a compelling seismic retrofitting technology. Designers can compare various retrofitting strategies based on building height and storeys to select the most efficient option.

## 2 Extended KDamper Concept

### 2.1 Overview of the EKD Absorber

The examined passive vibration absorption concept, illustrated in Fig. 1 and labeled as the EKD system [24], is an extension of the original KDamper concept.

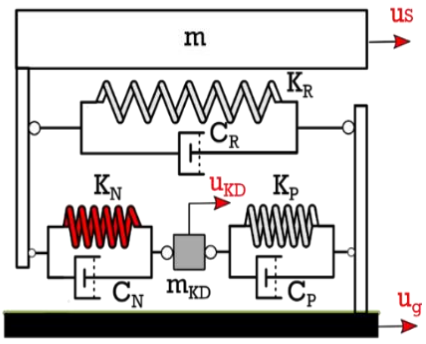


**Fig. 1.** Schematic presentation of the Extended KDamper (EKD) absorber excited at its base.

Similar to the QZS oscillator, a negative stiffness (NS) element is introduced. The NS element is attached to the primary and additional masses, and an additional positive stiffness element connects the added mass to the base. In contrast to the QZS, the primary essential condition for the KDamper (and its variants) is to maintain overall static and dynamic stability. The total equivalent stiffness of the system can be maintained at any desired level, as calculated in Eq. (1):

$$K_R + \frac{K_P K_N}{K_P + K_N} = K_0 = (2\pi f_0)^2 \left(m + m_{KD}\right) \tag{1}$$

The EKD system integrates an additional mass connected to a primary oscillator through a combination of negative stiffness (NS) and positive stiffness elements, while also incorporating artificial dampers. However, the primary distinction lies in the system configuration. In the EKD system, the damper added mass ($m_{KD}$) is linked to the base via a positive stiffness spring ($K_P$), while the negative stiffness element ($K_N$) is positioned between the damper's mass ($m_{KD}$) and the oscillating mass ($m$). Additionally, an extra artificial damper is introduced, positioned in parallel with the negative stiffness element. Consequently, the system includes two stiffness elements and dampers, identified as $K_P$ and $K_N$ and $C_P$ and $C_N$, respectively. Employing a simplifying approximation, the system can be treated as linear, suggesting that the negative stiffness (NS) element generates a force proportional to the relative displacement between its terminals. The governing equations of motion for the EKD system under base excitation is formulated as follows:

$$\begin{aligned} &m\ddot{u}_{S,rel} + C_R\dot{u}_{S,rel} + C_N(\dot{u}_{s,rel} - \dot{u}_{KD,rel}) + K_R u_{S,rel} + K_N(u_{s,rel} - u_{KD,rel}) = -m\ddot{u}_g \\ &m_{KD}\ddot{u}_{KD,rel} + C_N(\dot{u}_{KD,rel} - \dot{u}_{S,rel}) + C_P\dot{u}_{KD,rel} + K_N(u_{KD,rel} - u_{S,rel}) + K_P u_{KD,rel} = -m_{KD}\ddot{u}_g \end{aligned} \tag{2}$$

where $u_{s,rel}=u_s-u_g$ and $u_{KD,rel}=u_{KD}-u_g$.

### 2.2 Experimental prototype & proof of concept

Recently, an experimental prototype of the Extended version of the KDamper (EKD) was designed, constructed, and tested on the shaking table of the Soil Mechanics Laboratory of the National Technical University of Athens. The experiment functions as validation and proof of concept of the initial analytical and numerical frameworks [39]. The simplified experimental setup, depicted in Fig. 2, incorporates various components such as steel plates, aluminum parts, roller bearings, and a prismatic pre-stressed coil spring, employed for the realization of the NS element.

The design specifically aims for an oscillating mass ($m$) of approximately 16 kg (primary structure), with an internal added mass ($m_{KD}$) of around 0.82 kg, constituting 5% of the total mass ($m$). The prototype is constructed based on a constrained engineering-criteria based optimization methodology. Furthermore, additional calculations are performed to ensure structural members resist buckling, and relative displacements of device parts (e.g., maximum internal mass displacement, maximum negative stiffness relative displacement, maximum lever arm rotation, etc.) fall within predefined design limits. In the pursuit of exclusively assessing the efficiency of this negative stiffness (NS)-based mechanism, without considering the potential impact of additional damping, no artificial dampers were introduced to the device, further validating its vibration absorption capabilities.

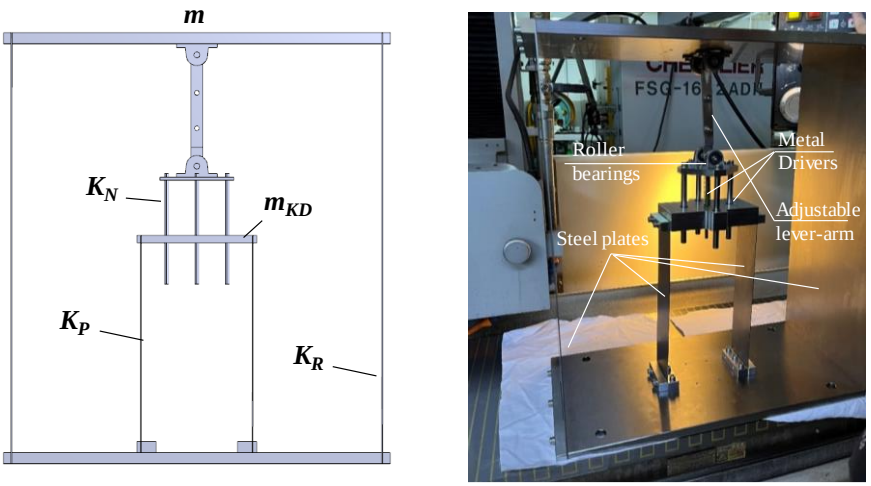


**Fig. 2.** Schematic presentation of the Extended KDamper (EKD) absorber excited at its base.

In Fig. 3, the experimentally estimated frequency response of the EKD vibration absorber is juxtaposed to the response of an equivalent Single Degree of Freedom (SDoF) oscillator. The obtained results provide validation for the expected behavior of the KDamper, thereby confirming the accuracy of the analytically derived equations of motion and dynamic performance.

Notably, when examining the magnification factor of the system, particularly when the seismic mass ($m$) is exclusively mounted on the $K_R$ stiffness elements (indicated by the black dashed-line), the efficacy of the system is highlighted. More specifically, there is an approximate 60% reduction in the fundamental resonance peak, highlighting the significant increase of the controlled systems equivalent damping, leading to an isolation frequency of approximately 1.4 Hz, aligning seamlessly with the intended objective of the device.

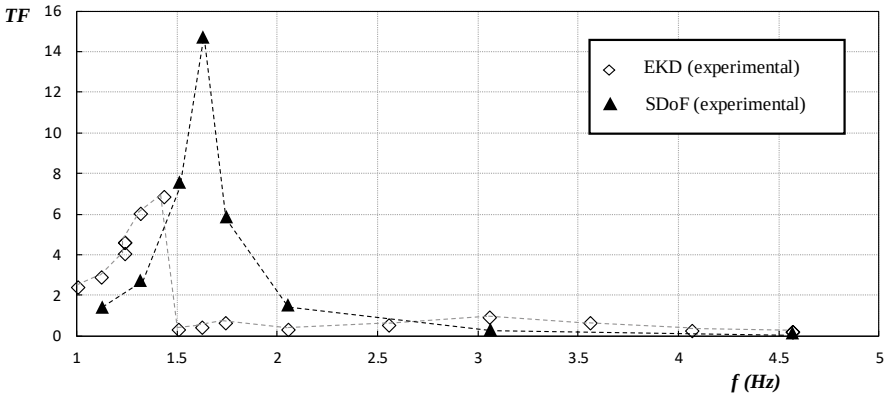


**Fig. 3.** Frequency response of the EKD device compared to the SDoF oscillator.

## 3 Optimization approach and performance assessment

The primary emphasis in designing the EKD is on determining the dimensions of its stiffness elements. While theoretically these values can be computed based on the equivalent static stiffness of the EKD setup, Eq. (1), practical implementation necessitates considerations such as adherence to manufacturing tolerances and thorough attention to nonlinearity [43]. To ensure both static and dynamic stability of the EKD, the design treats $K_P$, $K_N$, and $K_R$ as design parameters with adjustable values. Introducing perturbations $\varepsilon_P$, $\varepsilon_N$, and $\varepsilon_R$ to the stiffness variables $K_P$, $K_N$, and $K_R$, respectively, allows for the computation of the configuration's sensitivity in terms of stiffness instabilities. Instability occurs when the determinant of the stiffness matrix is equal to zero:

$$\det\left([K]_{static}\right)=0 \Rightarrow \left(1-\varepsilon_R\right)K_R+\frac{\left(1-\varepsilon_P\right)K_P\left(1+\varepsilon_N\right)K_N\left(u_{NS}=0\right)}{\left(1-\varepsilon_P\right)K_P+\left(1+\varepsilon_N\right)K_N\left(u_{NS}=0\right)}=0 \tag{3}$$

It's important to note that by ensuring the stability of the EKD in static conditions ($u_{NS}$ = 0), dynamic stability is also guaranteed. This is attributed to the mechanics of the NS configuration employed, where the highest absolute value of the generated NS is observed at the equilibrium position. Consequently, the positive stiffness elements $K_P$ and $K_R$, are derived as functions of $f_0$, and $K_N$. Assuming that the mass $m_{KD}$, the mass matrix of the initial structure to be controlled, the horizontal stiffness of the flexural elements of the floors $K_1$, …, $K_N$ .and the stability factors $\varepsilon_P$, $\varepsilon_N$, and $\varepsilon_R$ are known, the (free) independent design variables sought in the optimization process are as follows: (i) nominal frequency $f_{0,}$ (ii) NS element value $K_{N,}$ and (iii) damping coefficients $C_N$ and $C_{P.}$

With the equations of motion Eq. (1) and the free design variables of the EKD established, the objective is to obtain an optimal set of EKD parameters aiming to reduce the dynamic responses of the superstructure. Simultaneously, it is crucial to ensure that the maximum accelerations remain below a predetermined percentage of the peak ground acceleration (filter). Hence, the mechanism serves a dual purpose by aiming to reduce both floor drifts and floor absolute accelerations. The EKD design follows a constrained engineering criterion-driven optimization approach [24]. This approach considers the geometrical and constructional limitations, such as the NS stroke, imposed by the respective structural system, and retains the values of its individual components within reasonable ranges. The Harmony Search (HS) algorithm, a novel metaheuristic algorithm, is utilized [44],to determine the optimum values of the design parameters $K_N$, $f_0$ and $C_N$ and $C_P$ , assuming that the additional mass $m_{KD}$ factors $\varepsilon_P$, $\varepsilon_N$, and $\varepsilon_R$ are known. It is important to note that the optimal EKD set of parameters obtained by the proposed optimization methodology corresponds to the specific initial structure, and thus no analytical formulations can be derived for the EKD design.

Regarding the incorporation of parameters into the HS algorithm, a common approach involves adopting values frequently encountered in relevant literature, such as HMS=75, HMCR=0.5, and PAR=0.1. The optimization procedure uses an excitation input selected from a database of artificial accelerograms [24] designed to be spectrum-

compatible with the EC8 (spectral acceleration 0.36 g, ground type C, spectrum type I, and importance class II). Fig. 4 illustrates a sample artificial accelerogram, and the generated spectrum, compared to the EC8. Based on the feasibility and technological constraints imposed in the analysis, appropriate ranges are attributed to both the design variables of the optimization problem, as well as to the yielded dynamic responses.

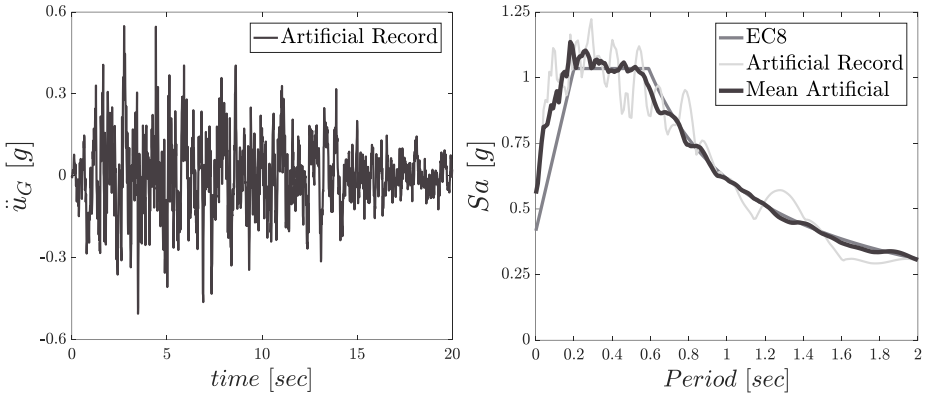


**Fig. 4.** (a) Artificial accelerogram, and (b) mean acceleration spectrum compared to the EC8.

The EKD devices are optimized according to the optimization methodology presented previously with the artificial accelerograms in order incorporate the EC8 provisions in the design process. To confirm the effectiveness of the seismic retrofit strategies and assess the dynamic behavior of the structures, a set of eight (8) real earthquake motions is utilized as input seismic excitation. These chosen records, sourced from the US, European, and Asian regions, encompass a diverse array of crucial seismic features, including Peak Ground Acceleration (PGA), magnitude (Mw), wide frequency spectrum, duration, and the count of notable acceleration cycles. Detailed information about the seismic characteristics of the selected excitations can be found in Table 1.

**Table 1.** Seismic characteristics of the selected real earthquake records.

| No | Earthquake | Year | Station | Ground Motion | Mw | PGA (g) | PGA/PGV (gsec/m) | $R_{JB}$ (km) | $Dur_{5\text{-}75\%}$ (sec) |
|---|---|---|---|---|---|---|---|---|---|
| 1 | Northridge | 1994 | N Hollywood | Near fault | 6.69 | 0.3087 | 1.4389 | 7.89 | 7.0 |
| 2 | L'Aquila | 2009 | V. Aterno | Near fault | 6.3 | 0.4018 | 1.2548 | 0.0 | 4.7 |
| 3 | Kocaeli | 1999 | Izmit | Near fault | 7.51 | 0.1651 | 0.7396 | 3.62 | 8.2 |
| 4 | Tabas | 1978 | Tabas | Near fault | 7.35 | 0.8540 | 0.8639 | 1.79 | 8.3 |
| 5 | Kobe | 1995 | Amagasaki | Near fault | 6.9 | 0.2758 | 0.8214 | 11.34 | 6.9 |
| 6 | Landers | 1992 | Joshua tree | Near fault | 7.28 | 0.2736 | 1.0125 | 11.03 | 21.7 |
| 7 | Duzce | 1999 | Lamont 1059 | Near fault | 7.14 | 0.1524 | 1.1844 | 4.17 | 10.4 |
| 8 | Friuli | 1976 | Tolmezzo | Near fault | 6.5 | 0.3571 | 1.5629 | 14.97 | 2.5 |

## 4 Implementation of the EKD at the base level of the structure

In this section, an EKD device is implemented at the base level of a multi-story building structure as a seismic protection/retrofitting measure, as illustrated in Fig. 5. This approach is straightforward, as the placement of the EKD is predetermined, and thus the optimization process is simplified. The EKD components are the stiffness elements and artificial dampers $K_N$-$C_N$ and $K_P$-$C_P$. It is noted that no stiffness element is placed in parallel to the original stiffness of the structure. The superstructure is modeled as a lumped mass system, with uniform masses and stiffnesses for all floors ($m_F$ = 360 *tn*, $k_F$ = 650 *MN/m*). The structure represents a typical medium-sized building whose floor weights correspond to about 400 $m^2$ of floor area, and the height of each story is assumed 3.2 *m*. Modal damping is considered, with a damping ratio of 2% for all modes.

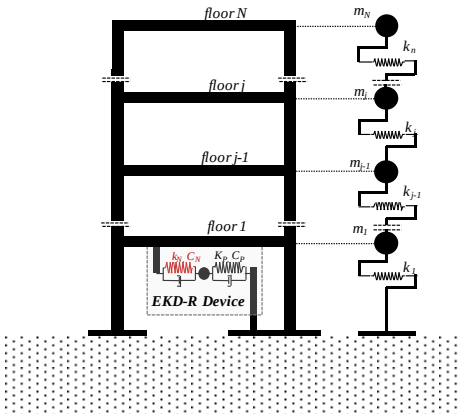


**Fig. 5.** Schematic representation of the EKD implemented at the base level of a multi-story structure, along with the lumped mass model of the superstructure.

The structure nominal base frequency controlled with the EKD can be expressed as:

$$K_0 = K_F + \frac{K_P K_N}{K_P + K_N} = \left(2\pi f_0\right)^2 m_{tot}$$
$$m_{tot} = \sum_1^N \left(M_{F,i}\right) + m_{KD} \tag{4}$$

The EKD introduces a negative stiffness element to the base level of the structure. The stability of the structure is ensured by properly selecting the stiffness elements of the EKD according to Eq. (4). However, to avoid significant alterations in the structural properties of the initial uncontrolled building and thus further ensure its stability, the nominal EKD frequency $f_0$ is selected to vary in the range of:

$$\left(\frac{2}{3}\right)\sqrt{\frac{K_F}{m_F}} \le \omega_0 = 2\pi f_0 \le \left(\frac{4}{3}\right) \times \sqrt{\frac{K_F}{m_F}} \tag{5}$$

Thus, the number of design variables of this retrofit strategy are four and can be obtained following the optimization methodology presented previously. To better understand the EKD dynamic behavior, the damping ratios of the $C_N$ and $C_P$ are defined as:

$$\zeta_N = \frac{C_N}{2\sqrt{K_0\left(M_F + m_{KD}\right)}}$$
$$\zeta_P = \frac{C_P}{2\sqrt{K_0\left(M_F + m_{KD}\right)}} \tag{6}$$

Three test cases are considered to examine the efficiency of the proposed retrofit strategy with the EKD: a 5-story, a 10-story, and a 15-story structure, representing low-rise, mid-rise, and high-rise buildings, respectively. In Table 2, the optimized parameters and the damping ratios of the artificial dampers of the EKD device are provided for all the examined test cases. The EKD mass implemented at the base of the structure is assumed 0.1% of the total structure mass. Finally, the variation foreseen in the values of the stiffness elements $K_P$, $K_R$, and $K_N$ is assumed 2, 2, and 5%, respectively.

**Table 2.** Optimized parameters of EKD device implemented at the base level of the structure.

| Test case | $f_0$ (*Hz*) | $K_N$ (*MN/m*) | $K_P$ (*MN/m*) | $C_N$ (*kNs/m*) | $\zeta_N$ (*%*) | $C_P$ (*kNs/m*) | $\zeta_P$ (*%*) |
|---|---|---|---|---|---|---|---|
| 5-story | 4.78 | -92.8 | 130.1 | 4989.1 | 0.229 | 412.3 | 0.021 |
| 10-story | 4.91 | -69.2 | 89.2 | 4994.6 | 0.2231 | 385.7 | 0.022 |
| 15-story | 5.11 | -55.2 | 65.84 | 4781.6 | 0.2038 | 487.3 | 0.0208 |

In Fig. 6, the dynamic responses of the controlled structures with the EKD at the base are presented for an EC8 spectrum-compatible artificial accelerogram, for all the examined test cases, and are compared to the uncontrolled structure (NC). The EKD

manages to significantly reduce the superstructure's dynamic response (drifts and absolute accelerations) for the low-rise structure, however, as the number of floor increases, its performance diminishes. To assess the performance of the proposed seismic upgrade methodology, the EKD system is also subjected to 8 real earthquake records, provided in Table 1. Fig. 7 presents the maximum values of the dynamic responses of the EKD structure, compared to the NC one, in the form of bar charts. The floor drifts and absolute accelerations are significantly reduced in the case of the 5-story structure, and again it is observed that the EKD is less effective for more flexible structures.

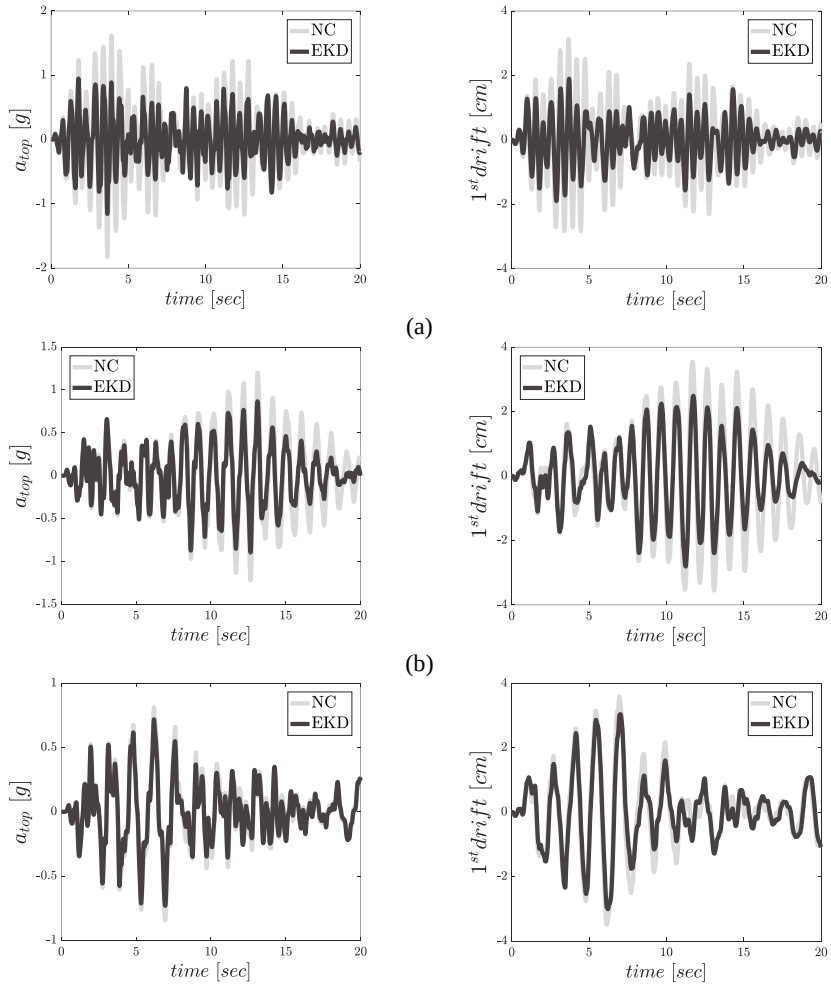


**Fig. 6.** Comparative dynamic response results (time histories) of the controlled multi-story structures with EKD device at its base (left: top floor absolute acceleration $a_{top}$, right: first floor drift *1st drift*), compared to the NC, for an EC8-compatible artificial accelerogram. (a) 5-story, (b) 10-story, and (c) 15-story buildings.

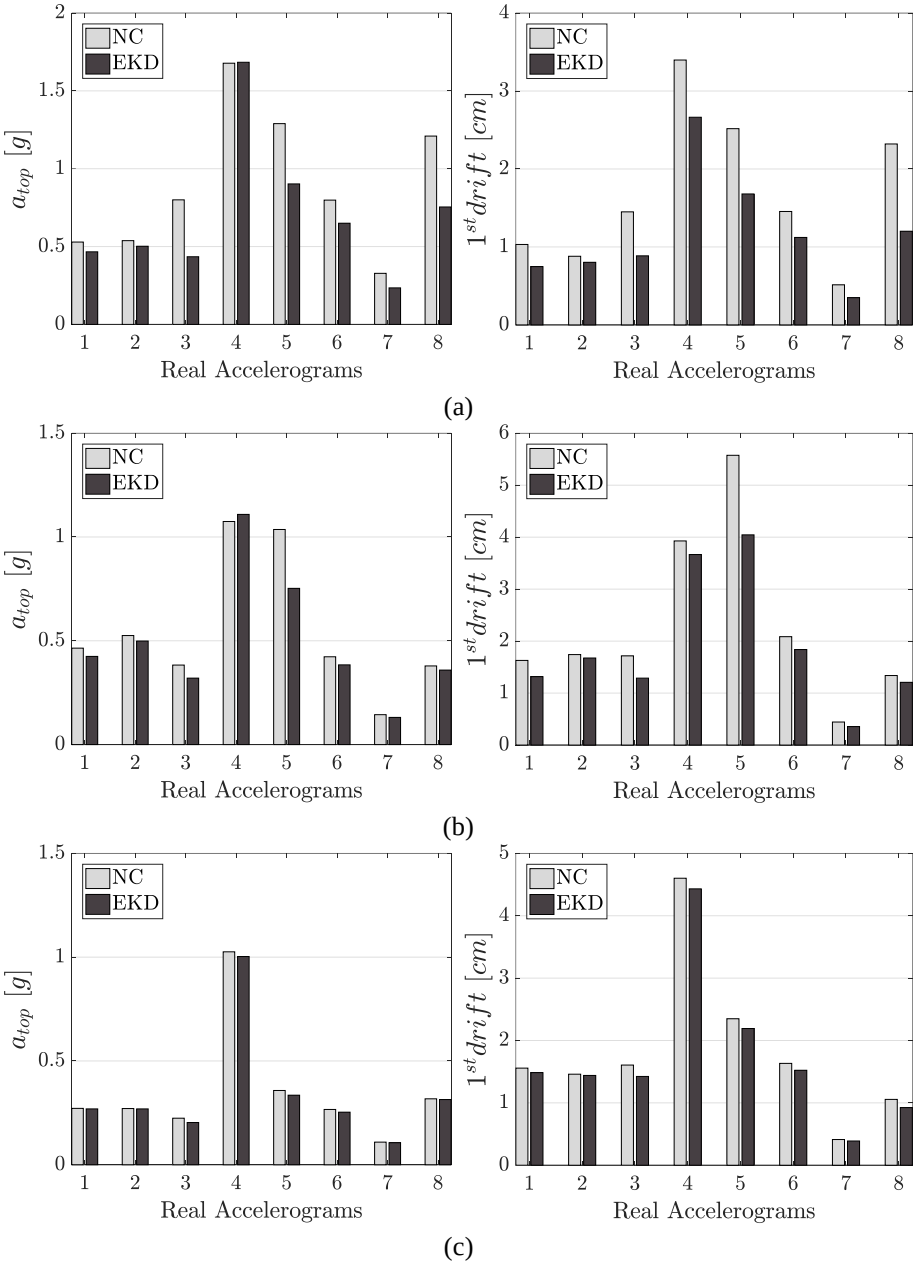


**Fig. 7.** Comparative dynamic response results (maximum values) of the controlled multi-story structures with EKD device at its base (left: top floor absolute acceleration $a_{top}$, right: first floor drift *1st drift*), compared to the NC, for all the selected real earthquake records. (a) 5-story, (b) 10-story, and (c) 15-story buildings.

## 5 Distribution of EKD devices along the height of the structure

An alternative, and more computationally demanding seismic retrofit approach, is to distribute a number of EKD devices along the height of the multi-story building structure, enabling the control of higher modes. The retrofit elements of each EKD device are the stiffness and damping elements $K_N$-$C_N$ and $K_P$-$C_P$. The total added mass is the same with the previous seismic protection approach, in order to have an equal comparison basis for the numerical results. The multi-story structures to be controlled are modeled as lumped mass systems and have the same properties as the ones presented in the previous retrofit strategy (Section 4). A schematic representation of this seismic upgrade method is presented in Fig. 8, where an EKD device is implemented between two consecutive floors (j) and (j-1).

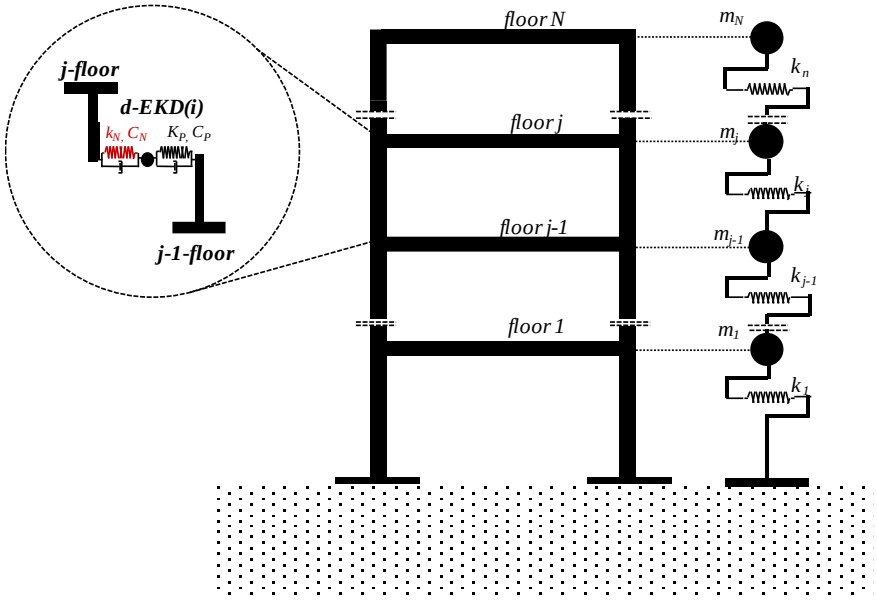


**Fig. 8.** Implementation of a EKD device (number *i*) between two consecutive floors (*j*) and (*j-1*) of the multi-story building structure.

By introducing the EKD negative stiffness mechanism (device number i) between two consecutive floors (j) and (j-1), the equivalent stiffness of the (j) floor is modified, and can be expressed as follows:

$$K_{F,eq}^{j} = K_F^j + \frac{K_P^i K_N^i}{K_P^i + K_N^i} = \left(2\pi f_F^j\right)^2 \left(M_F + m_{KD}\right) \tag{7}$$

The proposed approach introduces negative stiffness elements distributed along the height of the structure, and thus, it is necessary to ensure the stability of each floor, and

as a result, the structures. For this reason, the equivalent nominal frequency of the (j) floor is selected to vary in the range:

$$\left(\frac{2}{3}\right)\sqrt{\frac{K_F}{m_F}} \le \omega_F^j = 2\pi f_F^j \le \left(\frac{4}{3}\right)\times\sqrt{\frac{K_F}{m_F}} \tag{8}$$

The number of free design variables per device is in this case also four (4), and the spatial allocation of the devices is set as a variable, ranging from the first up to the top floor of the building structure. As a result, each EKD device has five (5) design variables. The optimal design of the proposed retrofit strategy follows the optimization methodology presented in Section 3. The same three test cases are examined, in order to verify the effectiveness of this approach to low, mid, and high-rise buildings. In Table 3, the optimal values of all EKD components, along with the optimum placement of the devices, are presented. It is noted that since the EKD devices are distributed along the height of the structure, large additional masses are undesirable, and thus, the sum of the EKD additional masses is 0.1% of the total superstructure mass. Finally, the variation foreseen in the values of the negative stiffness elements ($\varepsilon_N$) is assumed 10%.

**Table 3.** Optimized parameters and spatial allocation of the implemented EKD devices along the height of the building structure.

| Test case | #Device/ floor | $f_0$ (*Hz*) | $K_N$ (*kN/m*) | $K_P$ (*kN/m*) | $C_N$ (*kNs/m*) | $\zeta_N$ (*%*) | $C_P$ (*kNs/m*) | $\zeta_P$ (*%*) |
|---|---|---|---|---|---|---|---|---|
| 5-story | #1/floor 2 | 5.023 | -81.55 | 113.2 | 4625.5 | 13.14 | 114.2 | 1.3 |
| | #2/floor 1 | 5.435 | -47.99 | 60.63 | 4124.1 | 12.14 | 381.5 | 2.1 |
| | #3/floor 3 | 5.037 | -74.01 | 99.43 | 3824.3 | 13.10 | 563 | 2.8 |
| 10-story | #1/floor 4 | 5.067 | -62.71 | 80.39 | 4997.3 | 12.16 | 16.3 | 1.2 |
| | #2/floor 5 | 4.983 | -67.51 | 87.36 | 3824.5 | 10.3 | 427.1 | 2.8 |
| | #3/floor 6 | 5.116 | -79.74 | 111.82 | 4624.2 | 13.64 | 269.4 | 2.2 |
| 15-story | #1/floor 5 | 5.011 | -65.86 | 84.95 | 4673.4 | 13.68 | 463.2 | 2.8 |
| | #2/floor 6 | 4.97 | -66.88 | 86.17 | 4173.9 | 11.75 | 389.4 | 2.3 |
| | #3/floor 2 | 5.027 | -65.79 | 85.04 | 3994.7 | 10.34 | 210.8 | 1.9 |

Fig. 9 presents the time history responses of the controlled buildings with 3 EKD devices, distributed along the height of the building, for one artificial accelerogram, and are compared with the NC building. The proposed distributed approach effectively reduces the peak dynamic responses, in terms of drifts and absolute accelerations in all the examined test cases. The effectiveness of the distributed retrofit strategy is also verified with real earthquake records. In Fig. 10, the peak of the dynamic responses of the D-EKD and the NC structures are presented in the form of bar charts for all 8 ground motions presented in Table 1. The D-EKD manages to significantly reduce the seismic responses in the case of the low and mid-rise structures. It is worth noting that in the case of the high-rise structure, its dynamic behavior is also improved.

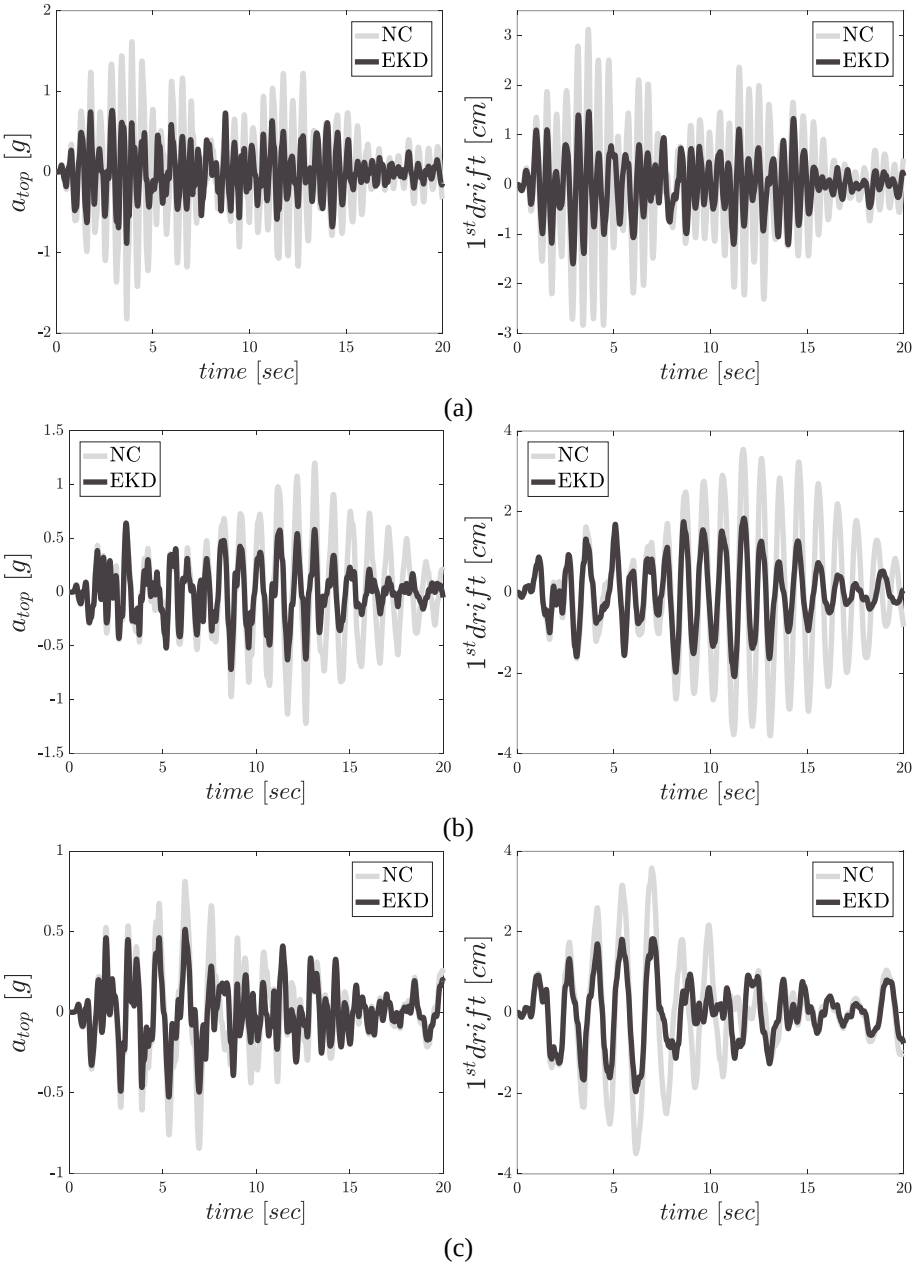


**Fig. 9.** Comparative dynamic response results (time histories) of the controlled multi-story structures with distributed EKD devices (left: top floor absolute acceleration $a_{top}$, right: first floor drift *1st drift*), compared to the IN, for an EC8-compatible artificial accelerogram. (a) 5-story, (b) 10-story, and (c) 15-story buildings.

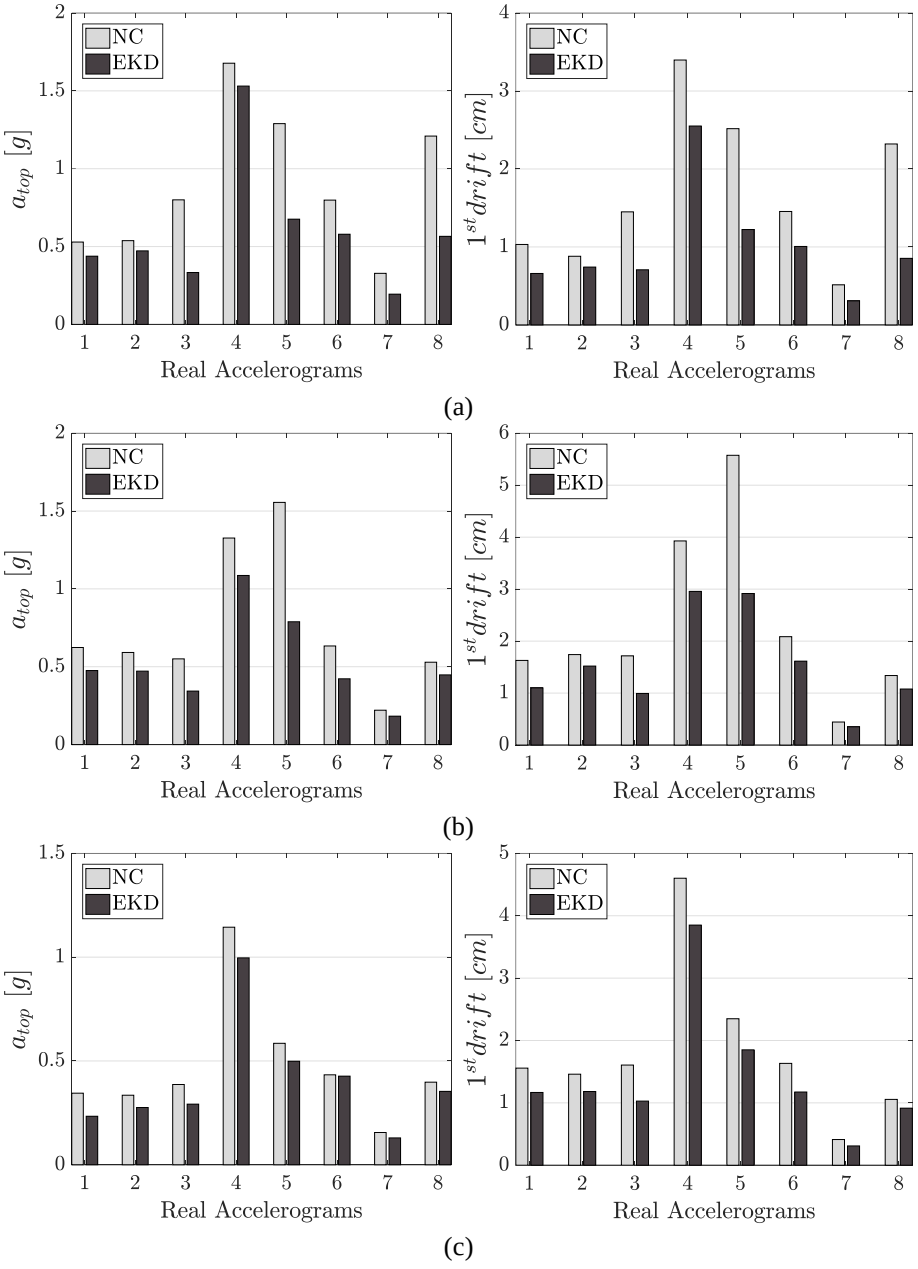


**Fig. 10.** Comparative dynamic response results (maximum values) of the controlled multi-story structures with distributed EKD devices (left: top floor absolute acceleration $a_{top}$, right: first floor drift *1st drift*), compared to the IN, for all the selected real earthquake records. (a) 5-story, (b) 10-story, and (c) 15-story buildings.

## 6 Conclusions

This paper investigates the performance of multi-story building structures that incorporate novel negative stiffness-based vibration absorbers (EKD), as seismic retrofitting measures. Three test cases of multi-story buildings are thoroughly investigated, representing low, mid and high-rise structures. Two distinct retrofit approaches are investigated, with the primary objective to provide insights into the effectiveness of each strategy based on the structure's height and number of stories, providing a comprehensive evaluation of the pros and cons of each option.

More specifically, the first approach presents the implementation of the EKD mechanism at the base of the structures. The design of this configuration is straightforward, significantly simplifying the optimization process of the employed device. As an alternative, a more computationally demanding seismic retrofit approach, is to distribute a number of EKD devices along the height of the multi-story building structure, enabling the control of higher modes.

The optimal parameters of the retrofit strategies are obtained following a constrained engineering-criteria driven optimization approach. In addition, the design process follows the provisions of the EC8 by selecting the excitation input from a database of EC8 spectrum-compatible artificial accelerograms. The performance of the controlled structures is finally assessed with real strong ground motions. Based on the dynamic analysis and the numerical results obtained, the following key concluding remarks may be summarized as follows:

i. The design of the EKD devices in both approaches is realistic, as it is based on a constrained optimization approach with proper constraints and limitations in the structural dynamic responses and EKD components values.
ii. The stability of the system is ensured, as the design foresees simultaneous variation in the values of all stiffness elements, including the one with negative constant, and avoids significant alterations in the structural properties.
iii. The retrofit strategy with the EKD implemented at the base of the structure manages to significantly reduce the peak responses of the low-rise building. However, this approach has proven to be less effective for flexible structures.
iv. The distribution of EKD devices along the height of the multi-story buildings significantly improves the seismic responses of the superstructure in the case of the low and mid-rise structures. It is also worth noting that in the case of the high-rise structure, the dynamic behavior is notably improved.

## 7 Acknowledgments

Konstantinos Kapasakalis would like to acknowledge the support by the Bodossaki Foundation – Scholarship for Postdoctoral studies. Antonios Mantakas and Moris Kalderon would like to acknowledge the financial support provided by the EU's Horizon 2020 research and innovation program under the Marie Sklodowska-Curie grant (Grant Agreement No. INSPIRE-813424, 'INSPIRE, Innovative Ground Interface Concepts for Structure Protection').

## References


1. Naeim F, Kelly JM. Design of seismic isolated structures: from theory to practice. John Wiley & Sons; 1999.
2. Symans MD, Charney FA, Whittaker AS, Constantinou MC, Kircher CA, Johnson MW, et al. Energy Dissipation Systems for Seismic Applications: Current Practice and Recent Developments. Journal of Structural Engineering 2007;134:3–21. https://doi.org/10.1061/(asce)0733-9445(2008)134:1(3).
3. Frahm H. Device for damping of bodies. US patent #989958, 1911.
4. Den Hartog JP. Mechanical Vibrations. 4th ed. New York: 1956. https://doi.org/10.1038/161503c0.
5. Kareem A. Mitigation of wind induced motion of tall buildings. Journal of Wind Engineering and Industrial Aerodynamics 1983;11:273–84. https://doi.org/10.1016/0167-6105(83)90106-X.
6. Elias S, Matsagar V. Optimum Tuned Mass Damper for Wind and Earthquake Response Control of High-Rise Building. Advances in Structural Engineering: Dynamics, Volume Two 2015:751–1616. https://doi.org/10.1007/978-81-322-2193-7.
7. Hoang N, Fujino Y, Warnitchai P. Optimal tuned mass damper for seismic applications and practical design formulas. Eng Struct 2008;30:707–15. https://doi.org/10.1016/J.ENGSTRUCT.2007.05.007.
8. Kareem A, Kijewski T, Tamura Y. Mitigation of motions of tall buildings with specific examples of recent applications. Wind and Structures, An International Journal 1999;2:201–51. https://doi.org/10.12989/WAS.1999.2.3.201.
9. Taniguchi T, Der Kiureghian A, Melkumyan M. Effect of tuned mass damper on displacement demand of base-isolated structures. Eng Struct 2008;30:3478–88. https://doi.org/10.1016/j.engstruct.2008.05.027.
10. Xiang P, Nishitani A. Optimum design for more effective tuned mass damper system and its application to base-isolated buildings. Struct Control Health Monit 2014;21. https://doi.org/10.1002/stc.1556.
11. De Domenico D, Ricciardi G. Earthquake-resilient design of base isolated buildings with TMD at basement: Application to a case study. Soil Dynamics and Earthquake Engineering 2018;113:503–21. https://doi.org/10.1016/j.soildyn.2018.06.022.
12. Kamgar R, Samea P, Khatibinia M. Optimizing parameters of tuned mass damper subjected to critical earthquake. The Structural Design of Tall and Special Buildings 2018;27:e1460. https://doi.org/10.1002/TAL.1460.
13. Khatibinia M, Gholami H, Kamgar R. Optimal design of tuned mass dampers subjected to continuous stationary critical excitation. Int J Dyn Control 2018;6:1094–104. https://doi.org/10.1007/S40435-017-0386-7/FIGURES/10.
14. Kamgar R, Gholami F, Zarif Sanayei HR, Heidarzadeh H. Modified Tuned Liquid Dampers for Seismic Protection of Buildings Considering Soil–Structure Interaction Effects. Iranian Journal of Science and Technology - Transactions of Civil Engineering 2020;44:339–54. https://doi.org/10.1007/S40996-019-00302-X/TABLES/5.
15. Dadkhah M, Kamgar R, Heidarzadeh H, Jakubczyk-Galczyńska A, Jankowski R. Improvement of Performance Level of Steel Moment-Resisting Frames Using Tuned Mass Damper System. Applied Sciences 2020, Vol 10, Page 3403 2020;10:3403. https://doi.org/10.3390/APP10103403.
16. Salimi M, Kamgar R, Heidarzadeh H. An evaluation of the advantages of friction TMD over conventional TMD. Innovative Infrastructure Solutions 2021;6:1–12. https://doi.org/10.1007/S41062-021-00473-5/FIGURES/7.

17. Nagarajaiah S, Sonmez E. Structures with Semiactive Variable Stiffness Single/Multiple Tuned Mass Dampers. Journal of Structural Engineering 2007;133:67–77. https://doi.org/10.1061/(asce)0733-9445(2007)133:1(67).
18. Weber B, Feltrin G. Assessment of long-term behavior of tuned mass dampers by system identification. Eng Struct 2010;32:3670–82. https://doi.org/10.1016/j.engstruct.2010.08.011.
19. Sladek JR, Klingner RE. Effect of TunedMass Dampers on Seismic Response. Journal of Structural Engineering 1983;109:2004–9. https://doi.org/10.1061/(ASCE)0733-9445(1983)109:8(2004).
20. Clark a. J. Multiple passive tuned mass damper for reducing earthquake induced building motion. 9th World Conference in Earthquake Engineering 1988:779–784.
21. Ayorinde EO, Warburton GB. Minimizing structural vibrations with absorbers. Earthq Eng Struct Dyn 1980;8:219–36. https://doi.org/10.1002/EQE.4290080303.
22. Chen G, Wu J. Optimal Placement of Multiple Tune Mass Dampers for Seismic Structures. Journal of Structural Engineering 2001;127:1054–62. https://doi.org/10.1061/(ASCE)0733-9445(2001)127:9(1054).
23. Antoniadis IA, Kanarachos SA, Gryllias K, Sapountzakis IE. KDamping: A stiffness based vibration absorption concept. JVC/Journal of Vibration and Control 2018;24:588–606. https://doi.org/10.1177/1077546316646514.
24. Kapasakalis KA, Antoniadis IA, Sapountzakis EJ. Constrained optimal design of seismic base absorbers based on an extended KDamper concept. Eng Struct 2021;226. https://doi.org/10.1016/j.engstruct.2020.111312.
25. Molyneaux W. Supports for Vibration Isolation. G. Britain: ARC/CP-322, Aer Res Council; 1957.
26. Carrella A, Brennan MJ, Waters TPÃ. ARTICLE IN PRESS Static analysis of a passive vibration isolator with quasi-zero-stiffness characteristic 2007;301:678–89. https://doi.org/10.1016/j.jsv.2006.10.011.
27. Sun T, Lai Z, Nagarajaiah S, Li HN. Negative stiffness device for seismic protection of smart base isolated benchmark building. Struct Control Health Monit 2017. https://doi.org/10.1002/stc.1968.
28. Sarlis AA, Pasala DTR, Constantinou MC, Reinhorn AM, Nagarajaiah S, Taylor DP. Negative Stiffness Device for Seismic Protection of Structures: Shake Table Testing of a Seismically Isolated Structure. Journal of Structural Engineering 2016. https://doi.org/10.1061/(asce)st.1943-541x.0001455.
29. Pasala DT, Sarlis A, Nagarajaiah S, Reinhorn A, Constantinou M, Taylor D. Adaptive Negative Stiffness: New Structural Modification Approach for Seismic Protection. Adv Mat Res 2013;639–640. https://doi.org/10.4028/www.scientific.net/AMR.639-640.54.
30. Kapasakalis KA, Antoniadis IA, Sapountzakis EJ. Performance assessment of the KDamper as a seismic Absorption Base. Struct Control Health Monit 2020;27. https://doi.org/10.1002/stc.2482.
31. Paradeisiotis A, Kalderon M, Antoniadis I. Advanced negative stiffness absorber for low-frequency noise insulation of panels. AIP Adv 2021;11:65003. https://doi.org/10.1063/5.0045937.
32. Kalderon M, Paradeisiotis A, Antoniadis I. A Meta-structure for Low-frequency Acoustic Treatment Based on a KDamper-Inertial Amplification Concept. Euronoise 2021, 2021, p. 1333–43.
33. Sapountzakis EJ, Syrimi PG, Antoniadis IA. KDamper Concept in Seismic Isolation of Bridges. In: Proc of the 1st ICONHIC 2016, Chania, Crete, Greece: 2016, p. 28–30.

34. Antoniou M, Alvertos A, Sapountzakis EJ, Anastasopoulos I. Application of the Extended KDamper to the Seismic Protection of Bridges: Design Optimization, Nonlinear Response, SSI and Pounding Effects. Journal of Earthquake Engineering n.d.:1–35. https://doi.org/10.1080/13632469.2023.2250463.
35. Kapasakalis KA, Antoniadis IA, Sapountzakis EJ, Kampitsis AE. Vibration Mitigation of Wind Turbine Towers Using Negative Stiffness Absorbers. Journal of Civil Engineering and Construction 2021;10:123–39. https://doi.org/10.32732/JCEC.2021.10.3.123.
36. Kampitsis A, Kapasakalis K, Via-Estrem L. An integrated FEA-CFD simulation of offshore wind turbines with vibration control systems. Eng Struct 2022;254:113859. https://doi.org/10.1016/J.ENGSTRUCT.2022.113859.
37. Kapasakalis KA, Alvertos AE, Mantakas AG, Antoniadis IA, Sapountzakis EJ. Advanced negative stiffness vibration absorber coupled with soil-structure interaction for seismic protection of buildings. Proceedings of the International Conference on Structural Dynamic , EURODYN 2020;2:4160–76. https://doi.org/10.47964/1120.9340.19963.
38. Mantakas AG, Kapasakalis KA, Alvertos AE, Antoniadis IA, Sapountzakis EJ. A negative stiffness dynamic base absorber for seismic retrofitting of residential buildings. Struct Control Health Monit 2022;29:e3127. https://doi.org/10.1002/STC.3127.
39. Mantakas A, Chondrogiannis KA, Kalderon M, Kapasakalis K, Chatzi E, Sapountzakis E, et al. Design and Experimental Verification of an Extended KDamper - Based Vibration Absorber. Proceedings of EURODYN 2023, EASD Procedia; 2023.
40. Kapasakalis K, Mantakas A, Kalderon M, Antoniou M, Sapountzakis EJ. Performance Evaluation of Distributed Extended KDamper Devices for Seismic Protection of Mid-Rise Building Structures. Journal of Earthquake Engineering 2023. https://doi.org/10.1080/13632469.2023.2226227.
41. Mantakas A, Kapasakalis K, Kalderon M, Antoniou M, Antoniadis IA, Sapountzakis E. 3D Numerical Investigation of an Extended KDamper Absorber for Seismic Retrofitting of Low-Rise Buildings. COMPDYN Proceedings 2023. https://doi.org/10.7712/120123.10453.20434.
42. Kapasakalis K, Mantakas A, Kalderon M, Antoniou M, Sapountzakis EJ. Performance Evaluation of Distributed Extended KDamper Devices for Seismic Protection of Mid-Rise Building Structures. Journal of Earthquake Engineering 2023. https://doi.org/10.1080/13632469.2023.2226227.
43. Li H, Li Y, Li J. Negative stiffness devices for vibration isolation applications: A review. Advances in Structural Engineering 2020;23:1739–55. https://doi.org/10.1177/1369433219900311.
44. Zong Woo Geem, Joong Hoon Kim, Loganathan GV. A New Heuristic Optimization Algorithm: Harmony Search. Simulation 2001;76:60–8. https://doi.org/10.1177/003754970107600201.